



Original Paper

Carbon nanotube enhanced water-based drilling fluid for high temperature and high salinity deep resource development

Jing-Ping Liu^{a, **}, Xian-Fa Zhang^a, Wen-Chao Zhang^a, Kai-He Lv^a, Yin-Rui Bai^a,
Jin-Tang Wang^a, Xian-Bin Huang^a, Jia-Feng Jin^a, Jin-Sheng Sun^{a, b, *}

^a College of Petroleum Engineering, China University of Petroleum (East China), Qingdao 266580, China

^b CNPC Engineering Technology R&D Company Limited, Beijing 102206, China



ARTICLE INFO

Article history:

Received 11 November 2020

Accepted 5 January 2021

Available online 1 October 2021

Edited by Xiu-Qiu Peng

Keywords:

High temperature

Water-based drilling fluid

High salinity

Carbon nanotube

Deep resources

ABSTRACT

Drilling fluids face failure during drilling deep reservoir with high temperature and high salt. The experimental results show that high temperature and salinity reduce the negative charge on the surface of bentonite in the drilling fluid and cause the coalescence of bentonite particles. As a result, the particles coalesce, the grid structure is destroyed, and the rheological properties, rock-carrying capacity and filtration properties are lost. To resolve the foregoing, in this study, 0.05-wt% carbon nanotubes are introduced into a 4% bentonite drilling fluid under conditions where the temperature and concentration of added NaCl reach 180 °C and 10 wt%, respectively. The carbon nanotubes adsorb on the bentonite surface and increase the space among bentonite particles. The steric hindrance prevents the coalescence of bentonite in high temperature and high salt environment. Thus bentonite maintains the small size distribution of bentonite and supports the bentonite grid structure in the drilling fluid. As a result, the rock-carrying capacity of the drilling fluid increases by 85.1%. Moreover, the mud cake formed by the accumulation of small-sized bentonite particles is dense; consequently, the filtration of bentonite drilling fluid reduced by 30.2%.

© 2022 The Authors. Publishing services by Elsevier B.V. on behalf of KeAi Communications Co. Ltd. This is an open access article under the CC BY-NC-ND license (<http://creativecommons.org/licenses/by-nc-nd/4.0/>).

1. Introduction

With the rapid advancement of modern technology, energy consumption has increased significantly. One of the effective solutions to this problem is to increase the development of energy in deep formations. Gas and oil (Bera and Belhaj, 2016; Chen et al., 2019; Yu et al., 2019; Fu et al., 2020; Jalal et al., 2020), coal (Li et al., 2015; Xu et al., 2018), mineral (Tokimatsu et al., 2018), geothermal resources are abundant in deep earth (Anderson and Rezaie, 2019). Geothermal energy is clean and efficient and has been used worldwide. By 2050, geothermal resources will provide 3% of electricity generation (Shortall et al., 2015). The drilling and development of resources in deep formations are thus important research directions in petroleum engineering both at present and in

the future (De Silva et al., 2016; Li et al., 2016; Vedachalam et al., 2016). Reservoirs with a depth of more than 4.5 km are often referred to as deep reservoirs (Yang et al., 2019). Currently, the deepest reservoirs found are approximately 9 km, and the bottomhole temperature exceeds 180 °C (Aftab et al., 2017). Drilling is a necessary means of extracting reservoirs from deep formations (Pandey and Vishal, 2017; Willems et al., 2017; Saeid et al., 2018; Babaei and Hamidreza, 2019), and in the process of exploiting resources in deep formation, the drilling fluid, which first enters the formation, is the 'blood'. The drilling fluid is usually composed of bentonite, various chemicals, and weighting materials dispersed in water (Sehly et al., 2015). During the drilling process, the drilling fluid acts as carrying agent for weighting material and cuttings, balances formation pressure, transmits formation information, and lubricates drilling tools (Benayada et al., 2003; Baltoiu et al., 2008). The performance of drilling fluid is therefore a key to the effective extraction of resources in deep reservoirs.

Most deep formations are marked by high temperature and high salt content (especially NaCl) (Wu et al., 2014). At present, there is no clear definition of high temperature and high salt for drilling

* Corresponding author. College of Petroleum Engineering, China University of Petroleum (East China), Qingdao 266580, China.

** Corresponding author.

E-mail addresses: 20160038@upc.edu.cn (J.-P. Liu), sunjinsheng@upc.edu.cn (J.-S. Sun).

fluids, but a temperature of 150 °C is generally considered as high temperature, and temperatures above 180 °C or 200 °C are considered as ultra-high temperature. High salinity generally refers to salinity at saturation condition (Liu et al., 2018; Cui et al., 2020; He et al., 2020). Except for the three-sulfonic drilling fluid system, the conditions of 180 °C and 10% NaCl can be classified as high temperature and high salt, especially for the bentonite slurry (Guo et al., 2020; Tang et al., 2020). These conditions frequently increase fluid loss from the drilling fluid and deteriorate the rheology and lifting properties of this fluid (Shan et al., 2014; Amin and Hasan, 2018). This has resulted in numerous drilling accidents, such as wall collapse, stuck drilling, and even blowout, which can severely hinder the development of resources exploitation in deep formations. Some techniques include: reducing drilling fluids of the temperature on the ground, or preventing heat transfer between the annulus and fluids inside the drill string, which is used to prevent high temperature failure of the drilling fluid (Maury and Guenot, 1995), but it is difficult to achieve the desired effect. At present, the main technical problems exist in two aspects. The first is the failure mechanism of drilling fluid under high salinity conditions and high temperature. The second is the lack of a treatment agent that can enable the drilling fluid to simultaneously resist high salt concentration and high temperature.

In the study of drilling fluid inhibitors that are suitable under high temperature conditions, silicates are observed to effectively inhibit shale hydration and block shale pore (Guo et al., 2006; Yao et al., 2015; Yekeen et al., 2019; Liu et al., 2019). Potassium chloride has high hydration inhibition properties and is effective in inhibiting the hydration expansion of shale. HCOOK is also found effective in this regard (Yang et al., 2018). The surfactant compound can significantly inhibit the hydration expansion of shale and maintain the integrity of cuttings (Huang et al., 2017). Deep eutectic solvents synthesised by 3-phenylpropionic acid and choline chloride have excellent inhibitive properties for shale (Jia et al., 2019).

For water-based drilling fluids that are suitable at temperatures exceeding 180 °C, inhibitors, such as KCl, may be used because they are less affected by temperature. At high temperatures, however, the failure of suspending agents and filtration reducers frequently occur (Chu et al., 2013; Salami and Plank, 2013; Tiemeyer and Plank, 2013).

In the study of filtrate reducers and suspending agents for drilling fluids at high temperatures, fluid loss reducers, such as polymers, are usually degraded under high temperature conditions. This, therefore, affect the rheology, lifting and filtration of drilling fluids (Amin and Hasan, 2018).

For example, polyanionic cellulose and carboxymethyl cellulose, which are frequently degraded because of high temperatures, are not suitable for use in deep reservoirs (Menezes et al., 2010; Dias et al., 2015; Li et al., 2015). Acid-catalysed hydrolysis and redox reactions are mechanisms that cause polymer degradation. By adding antioxidants to inhibit the occurrence of these reactions, water-based drilling fluids can be stabilised at high temperatures (Wellington, 1983; Seright and Henrici, 1990; Vikas and Rajat, 2015). The formate, as an antioxidant, can increase the temperature resistance of polymers up to 175 °C. Polyethylene glycol can increase the temperature resistance of polymers in the drilling fluid up to 150 °C (Emmanuel et al., 2019). In continental Europe, when geothermal wells are drilled, xanthan gum is a commonly suspending agent for drilling fluids that ensures wellbore cleaning and carries debris (Timon and Johann, 2019). Water-soluble ionic liquids can effectively improve the rheology and fluid loss reduction performance of water-based drilling fluids under high temperature conditions (Luo et al., 2017).

At present, there are few studies on drilling fluids that are resistant to high temperatures and high salt concentrations. To

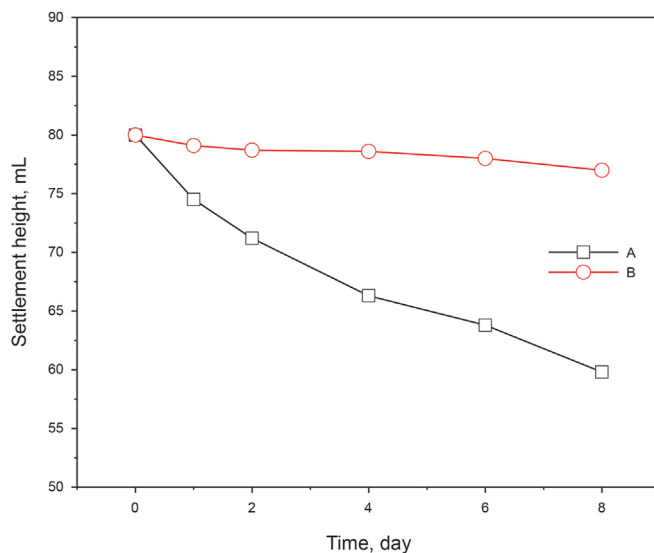


Fig. 1. Experiment of drilling fluid carrying rock cuttings. (a) 4% bentonite + 10% NaCl + barite ($\rho = 2.0 \text{ g/cm}^{-3}$) after ageing at 180 °C for 16 h; (b) 4% bentonite + 10% NaCl + 0.05% carbon nanotube + barite ($\rho = 2.0 \text{ g/cm}^{-3}$) after ageing at 180 °C for 16 h.

explore and develop the resources in deep formations, however, a breakthrough technology for drilling fluids is necessary and urgent. The covalent bond of C=C in carbon nanotubes is the most stable chemical bond in nature. As a new type of nanomaterial, carbon nanotubes are used in the fields of oil, electricity, heat, mechanics and hydrogen storage. The wall of carbon nanotubes is a carbon hexagonal network structure similar to graphite sheets, with each carbon adjacent to three surrounding carbon atoms. Nanotube materials thus have excellent temperature resistance and mechanical properties; moreover, they have extremely high strength and great toughness. In this work, the failure mechanism of water-based drilling fluid under high salt concentration conditions and high temperature is investigated. The performance of water-based drilling fluid that has been incorporated with carbon nanotubes under the aforementioned conditions is also examined. An intriguing phenomenon, which is observed under high salt conditions and high temperature, is that nanotube materials adsorb on the surface of bentonite particles in the drilling fluid. A strong steric hindrance effect among bentonite particles is created, and the fine particle size of these particles is maintained. These aid in

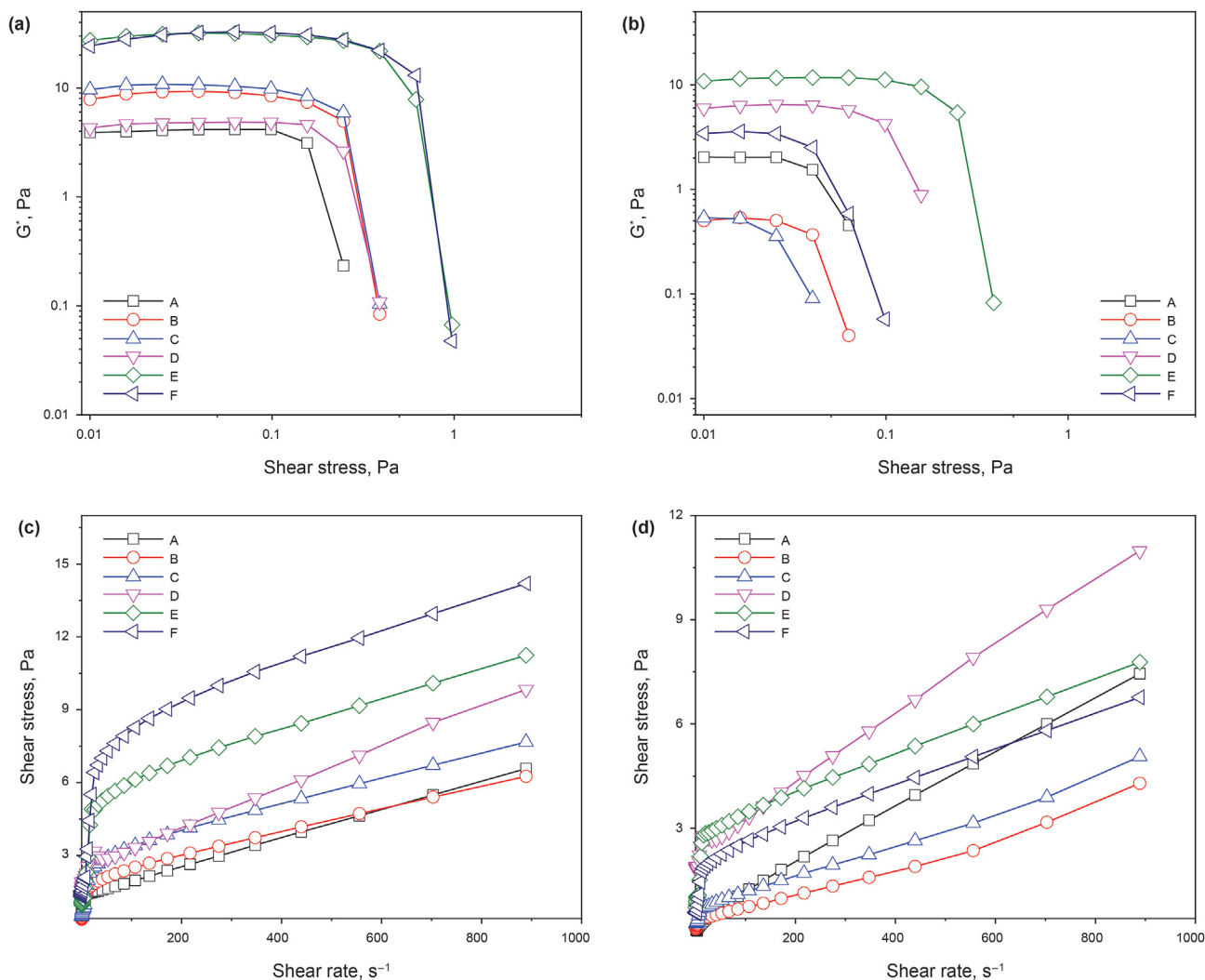


Fig. 2. Rheological diagram of drilling fluids. (a, b) Complex modulus (G^*) of drilling fluids as a function of stress ageing at 25 and 180 °C for 16 h; (c, d) Shear stress of drilling fluids as a function of shear rate ageing at 25 and 180 °C for 16 h. (A: 4% bentonite; B: 4% bentonite + 5% NaCl; C: 4% bentonite + 10% NaCl; D: 4% bentonite + 0.05% carbon nanotube; E: 4% bentonite + 5% NaCl + 0.05% carbon nanotube; F: 4% bentonite + 10% NaCl + 0.05% carbon nanotube).

maintaining the suspension characteristics and rheological properties of drilling fluids as well as prevent the loss of their filtration characteristics under high salt conditions and high temperature.

2. Experimental section

2.1. Materials

Bentonite and carbon nanotube (purity: >95%) are supplied by Chengdu Chunfeng Petroleum Technology Corporation (Sichuan, China). Carboxylated multi-arm carbon nanotubes are used in this paper with a diameter of 30–50 nm, a length of less than 10 μm , a carboxyl content of 0.73 wt%, and a specific surface area greater than 60 $\text{m}^2 \text{g}^{-1}$. The ultrasonic dispersion treatment is performed prior to the experiment, which makes its dispersibility even stronger. Barite ($\rho = 4.3 \text{ g/cm}^3$) is obtained from Anxian Huaxi Mineral Powder Corporation (Sichuan, China). NaCl (chemically pure) is purchased from Shanghai Maikelin Biochemical Technology Corporation.

2.2. Basic performance evaluation

Preparation of Water-Based Drilling Fluid. A 4% bentonite drilling fluid is prepared by first adding 4% (w/v) bentonite in deionised water. Thereafter, the fluid is stirred at 2000 rpm for 24 h (Cao et al., 2017). The materials described above is dissolved in the 4% bentonite drilling fluid and stirred at 2000 rpm for 20 min. It is then followed by an 8000-rpm stirring for 20 min. The fluid then undergoes static standing for 24 h to allow the materials to be thoroughly in contact with montmorillonite particles. To study the performance of the drilling fluid under high temperature, an ageing test is implemented in a GH-3-type roller oven (Qingdao Tongchun Petroleum Instrument Co., Ltd.) by rolling at 180 °C for 16 h.

Rheology Test. The rheological performance is investigated via a rheometer (Hake MARS III, Germany) with a coaxial cylinder sensor system (Li et al., 2017; Liu and Sheng, 2019). The test temperature is set at 25 °C. The shear rate is increased from 0.01 to 1000 s^{-1} in 300 s.

TEM Analysis. To better comprehend the microstructure of bentonite particles in drilling fluids, observations are made by transmission electron microscopy (TEM) with a JEOL-JEM1400Plus-type instrument (Hitachi Limited, Japan). The observations are

made at a 120-kV accelerating voltage. The sample is dropped on the copper net. After it is dried, we put it into the TEM for observation.

Zeta Potential Measurements. The effects of NaCl on the zeta potential of 4% bentonite drilling fluid are investigated using a Zetasizer-Nano-ZS90-type zeta potential analyser (Malvern Panalytical, U.K.) equipped with a microprocessor unit (Cao et al., 2017). Unless otherwise noted, all zeta-potential measurements are conducted at room temperature and repeated at least three times for each sample.

Particle Size Distribution Analysis. The bentonite size distributions in drilling fluids before and after ageing at 180 °C for 16 h are analysed using a Mastersizer-3000-type ultra-high speed intelligent particle size analyser (Malvern Panalytical, U.K.). The analysed

samples are obtained by adding 2 g of drilling fluid to 30 g of distilled water.

SEM Analysis. To better comprehend the filtration cake microstructure after the API fluid loss test, observations are made by scanning electron microscopy (SEM) using an EVO-15/LS-type instrument (Zeiss, Germany) (Liu et al. 2019, 2020). First, the filtration cake is slowly washed with deionised water and then dried in a vacuum oven at 45 °C for 24 h. The oven-dried sample is then cooled down in a desiccator at 25 °C until a constant mass is obtained. Finally, the filtrate cake is cut into samples with a length and width of about 1 cm, and spray gold, and micromorphology is observed by SEM with scanning voltage of 3.0 kV.

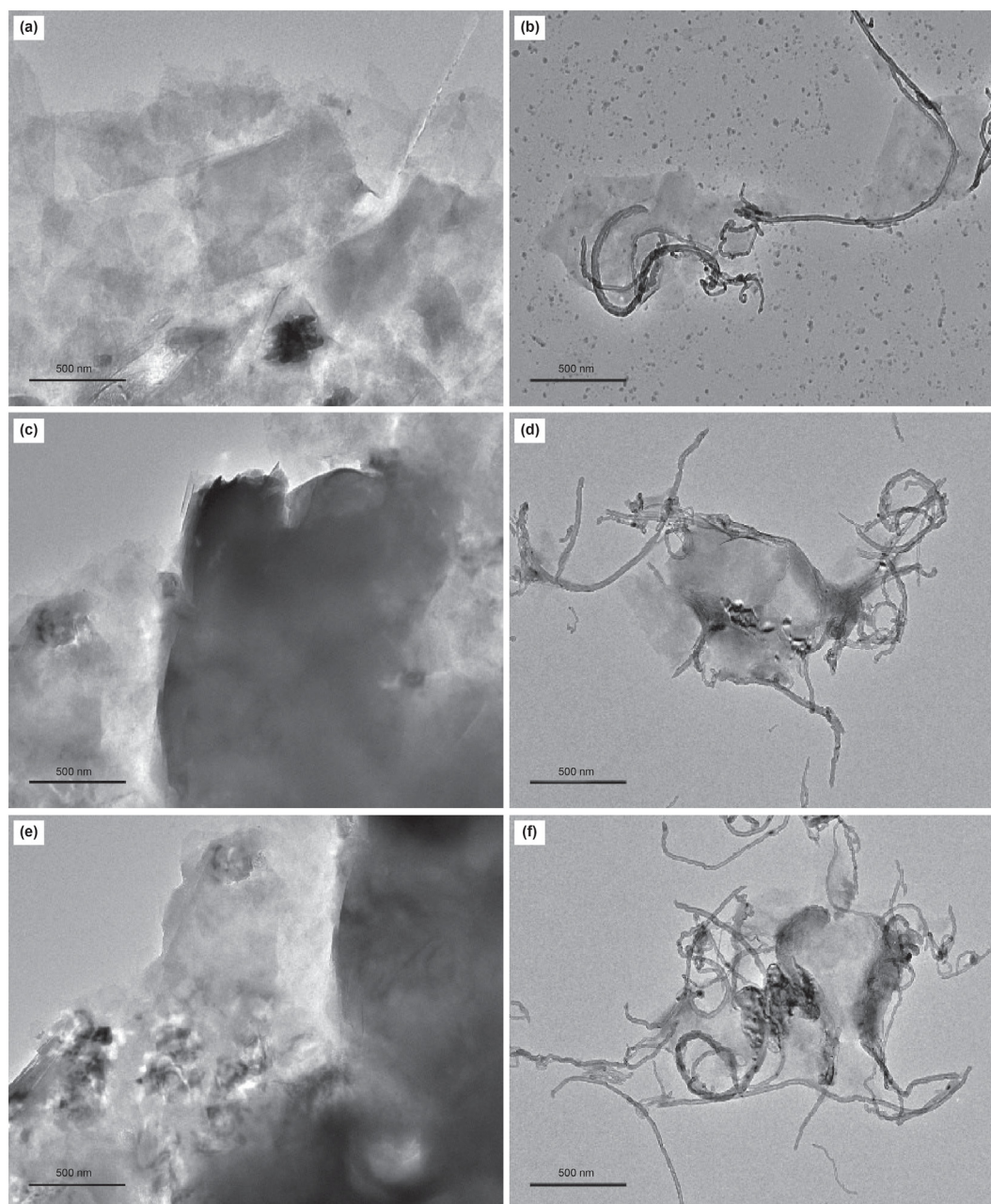


Fig. 3. TEM of drilling fluids after ageing at 180 °C for 16 h (a) 4% bentonite; (b) 4% bentonite +5% NaCl; (c) 4% bentonite +10% NaCl; (d) 4% bentonite +0.05% carbon nanotube; (e) 4% bentonite +0.05% carbon nanotube +5% NaCl; (f) 4% bentonite +0.05% carbon nanotube +10% NaCl.

2.3. Application performance evaluation

Lifting Measurements. The density of drilling fluid is increased to 2.0 g/cm^{-3} by barite. A 200-mL measuring cylinder is employed to measure 80 mL of this fluid, and the sedimentation height of the bentonite in this cylinder is observed and recorded at different times.

Measurement of water filtration by NMR. To qualitatively and quantitatively determine the water filtration through the pores in the core sample, nuclear magnetic resonance (NMR) T2 spectra test and magnetic resonance imaging are employed. The signals of hydrogen atoms with T2 relaxation can be identified by the NMR technology. The NMR analysis section (Macro MR12-150H-I, Niumag Analytical Instrument, Suzhou, China) is employed to scrutinise the core immersed in advance in different drilling fluids. The NMR detection and analysis system consists of a T2 spectrum section and an imaging section. Fluorocarbon oil is used as confining fluid with the thermostatic cycling system. The core holder is made of non-magnetic materials to eliminate the noise signal of experimental setups. In this experiment, waiting time (TW) is set to 2000 ms, accumulation times (NS) 64, echo time (Te) 0.35 ms, number of echoes (NECH) 12000. During imaging process, the accumulation time is set to 16, the preamplification (PRG) is selected to high, and the frequency coding step and phase encoding step are both set to 256.

American Petroleum Institute (API) Filtration Test. A filtration performance is conducted using a ZNZ-D3-type filtration apparatus (Qingdao Tongchun Petroleum Instrument Co., Ltd., China) according to the API guidelines for drilling fluids. A volume of drilling fluid is tested on the filter press equipped with a G50 Whatman quantitative filter paper at 0.7 MPa (Cao et al., 2017). When the API filter loss is measured and calculated, we only measure it at $t = 7.5 \text{ min}$, and then multiply by 2 to get the filter loss of 30min.

3. Results and discussion

3.1. Rheological properties and cutting-carrying characteristics of drilling fluids at high salinity and high temperature

As shown in Fig. 1, the drilling fluid density is increased to 2.0 g/

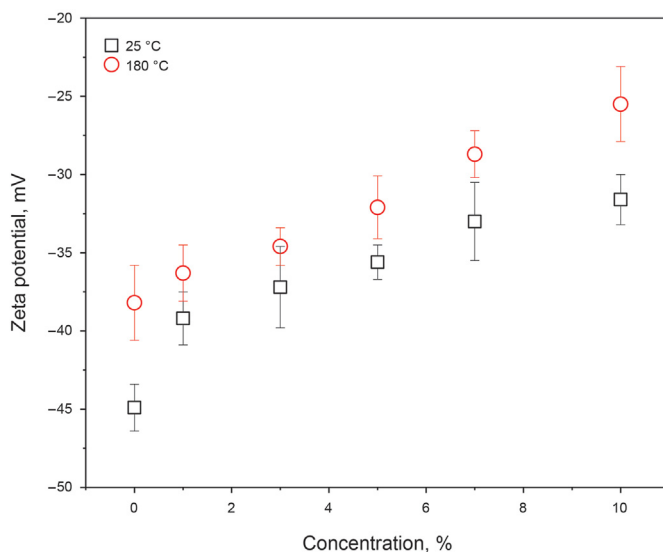


Fig. 4. Zeta potential of drilling fluid with 4% bentonite at different concentrations of NaCl at 25 °C and hot rolling for 16 h at 180 °C.

cm^{-3} with barite. After hot rolling at 180 °C for 16 h, the barite considerably settles over time in drilling fluid A with a sedimentation height of 20.2 mL. It shows that drilling fluid A cannot effectively carry or suspend weighting materials under high temperature and high salt conditions. This is because the grid structure in drilling fluid A is severely damaged by these conditions. If the drilling fluid cannot effectively carry the weighting materials or cuttings during drilling in the formation, then severe drilling card and pressure-bearing accidents will occur, causing major economic losses. The addition of 0.05 wt% carbon nanotubes to the drilling fluid significantly inhibits sedimentation. Only 3.0 mL of the barite settles, and the rock-carrying capacity of the drilling fluid is increased by 85.1%. This demonstrates that the addition of carbon nanotubes enables the 4% bentonite drilling fluid to effectively carry weighting materials or cuttings under high temperature and high salt conditions. Moreover, because the strength of the grid structure formed among bentonite particles is maintained, the addition of carbon nanotubes makes the application of drilling fluid in high temperature and high salt environments possible.

Fig. 2a and b shows the relationship between stress and the complex modulus (G^*) of drilling fluid. The high modulus (G_p^*) in which G^* is independent of stress is a linear viscoelastic region; all of the six drilling fluids exhibit linear viscoelastic regions (Li et al., 2015; Menezes et al., 2010). The value of G^* barely changes with the increase in stress until the critical stress is reached. The sudden drop in G^* means that the grid structure formed among the clay particles in the drilling fluid changes (Hunter and Alexander, 1963; Luckham and Rossi, 1999). This drop is in association with the static yield stress of the grid structure formed among clay particles. Here, critical stress shows the shear resistance of the grid structure. After the addition of NaCl to the drilling fluid with 4% bentonite, the fluid's shear resistance is improved, which may possibly be due to the addition of NaCl changing the connection model of clay particles. After hot rolling for 16 h at 180 °C, the shear resistance of G_p^* and the critical stress of drilling fluids B and C, which contain additions of NaCl, are substantially reduced. This indicates that high salt concentration and high temperature considerably damage the grid structure of drilling fluids. After the addition of carbon nanotubes, the values of G_p^* and the critical stress of drilling fluids under high temperature and high salt conditions are effectively maintained. This suggests that there must be a specific surface interaction between carbon nanotubes and bentonite particles in the drilling fluid. As a result, the grid structure is more stable, which makes it possible for the drilling fluid to withstand a higher applied stress and effectively adapt to high temperature and high salt conditions.

The shear stress of drilling fluid as the shear rate function is shown in Fig. 2c and d. With increasing shear rate, the shear stress of drilling fluids gradually increases, demonstrating the behaviour of plastic fluids. The six drilling fluids are all plastic fluids. When the shear stress is 0 Pa, the shear rate is not 0 s^{-1} . That is, they do not start to flow when a small magnitude of shear stress is applied, and to start the flow, a certain force must be introduced to destroy the continuous grid structure formed by the flocculation of bentonite particles in the drilling fluid. The minimum shear stress that can initiate flow is the static shear force. After hot rolling for 16 h at 180 °C, drilling fluids A, B, and C cease behaving as plastic fluids because there is basically no static shear force. The fluid, however, can start to flow with a slight shear stress, indicating that there is practically no continuous grid structure formed by bentonite particles in the drilling fluid. This renders the drilling fluid unsuitable under high salt conditions and high temperature in the formation. Drilling fluids D, E, and F, which have been added with carbon nanotubes, remain as plastic fluids, and all of them require a stress that is greater than the static shear force for the drilling fluid to

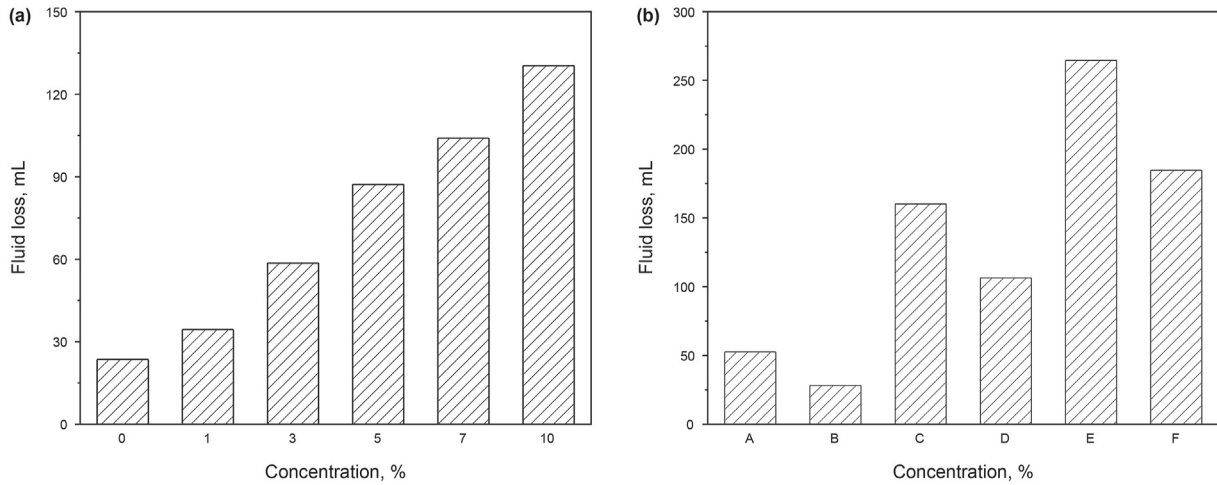


Fig. 5. (a) FL_{API} of 4% bentonite drilling fluid at different NaCl concentrations at 25 °C, and (b) FL_{API} of drilling fluids after hot rolling for 16 h at 180 °C (A, 4% bentonite; B, 4% bentonite + 0.05% carbon nanotube; C, 4% bentonite + 5% NaCl; D, 4% bentonite + 5% NaCl + 0.05% carbon nanotube; E, 4% bentonite + 10% NaCl; F, 4% bentonite + 10% NaCl + 0.05% carbon nanotube).

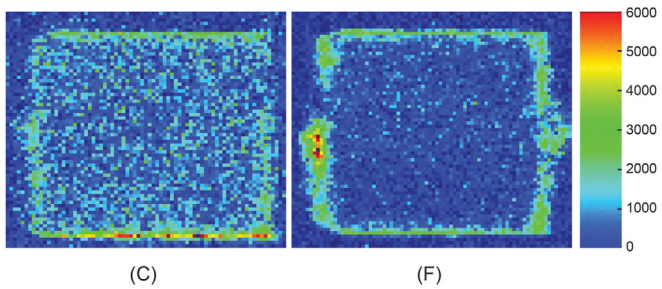
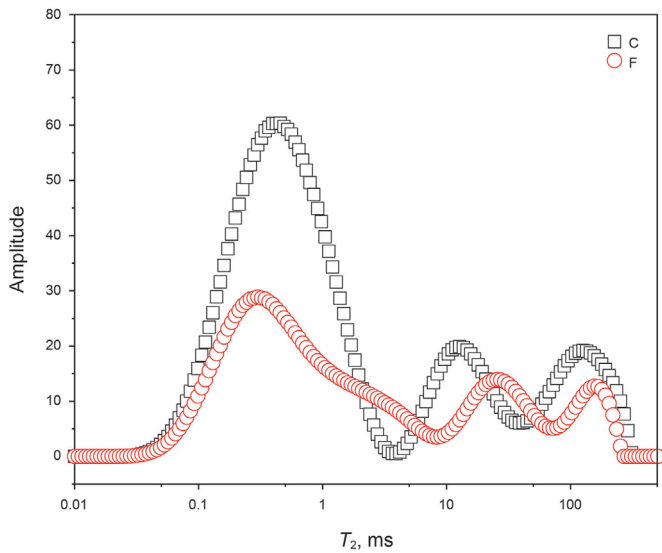


Fig. 6. Nuclear magnetic map of cores C and F after immersion in drilling fluids (C, immersion in 4% bentonite + 10% NaCl after hot rolling for 16 h at 180 °C; F, immersion in 4% bentonite + 10% NaCl + 0.05% carbon nanotube after hot rolling for 16 h at 180 °C). In the colour bar on the right, red colours indicate that the core is saturated with water.

flow. This indicates that the drilling fluid maintains a large number of continuous grid structures formed by bentonite particles under high temperature and high salt conditions. The formation of a continuous grid structure is essential for the drilling fluid to carry

and suspend rock debris in the formation (Kelessidis et al., 2011), and the carbon nanotubes make the drilling fluid suitable for the high temperature and high salt environment in deep formation.

Based on the above experimental results, it can be concluded that carbon nanotubes enable bentonite drilling fluids to exhibit excellent rheological properties under high temperature and high salt conditions. This improvement is possibly because of the formation of specific surface interactions between bentonite particles and carbon nanotubes in the drilling fluid. The question that accordingly arises is, what specific surface interactions between carbon nanotubes and bentonite particles make the bentonite drilling fluid resistant to high temperature and high salinity? To comprehend this, the microstructures of the six drilling fluids shown in Fig. 2 are examined by TEM, as shown in Fig. 3. Interestingly, a unique steric hindrance is observed among drilling fluids containing carbon nanotubes.

After hot rolling for 16 h at 180 °C, the bentonite particles in drilling fluids containing NaCl severely agglomerate (Fig. 3b and c). This may be because NaCl modifies the connection among bentonite particles and destroys the ability of the drilling fluid to carry cuttings and clean the wellbore. The foregoing is in sharp contrast to the reduction in Gp^* , as shown in Fig. 2b, and the fact that drilling fluids B and C have no static shear, as shown in Fig. 2d. It is evident that a considerable amount of carbon nanotubes added to the drilling fluid adsorb on bentonite particles. This adsorption introduces a strong steric hindrance and prevents the coalescence of bentonite particles under high temperature and high salt conditions. The particles thus remain in a dispersed state and maintain the grid structure in the drilling fluid. As a result, the drilling fluid is capable of withstanding high temperature and high salt concentration. Fig. 3d–f shows that as the amount of NaCl increases in the drilling fluid, the larger the amount of carbon nanotubes that adsorb on bentonite particles and the greater the steric hindrance among bentonite particles. The bentonite surface is negatively charged, and the edge of the particle is positively charged (Luckham and Rossi, 1999; Jung et al., 2011). When NaCl is added to the drilling fluid, it compresses the diffused double layer on the surface of bentonite particles, thus reducing the negative charge. On the other hand, because carbon nanotubes with large specific surface areas are negatively charged (experimental detection is -28.7 mV), they adsorb more easily on the edge of bentonite particles by electrostatic force.

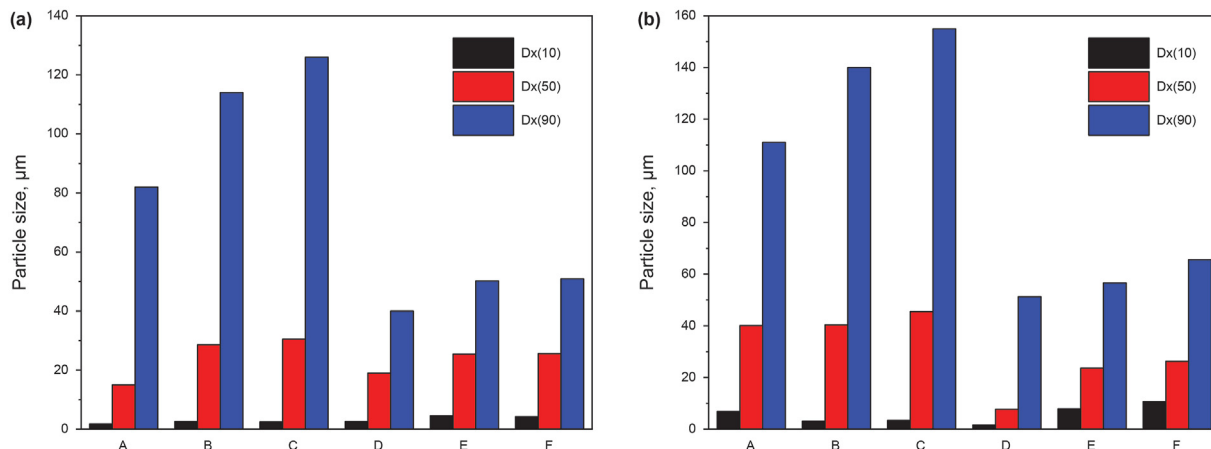


Fig. 7. (a) Size distribution of drilling fluids at 25 °C; (b) Size distribution of drilling fluids after 180 °C hot rolling for 16 h (A, 4% bentonite; B, 4% bentonite + 5% NaCl; C, 4% bentonite + 10% NaCl; D, 4% bentonite + 0.05% carbon nanotube; E, 4% bentonite + 0.05% carbon nanotube +5% NaCl; F, 4% bentonite + 0.05% carbon nanotube +10% NaCl).

In order to determine the change in the negative charge on the bentonite surface at high temperature and high NaCl concentration, the zeta potential of 4% bentonite drilling fluid at different NaCl concentrations is measured with a zeta potential meter, as shown in Fig. 4. At 25 °C, as the concentration of NaCl increases from 0 to 10 wt%, the negative charge on the bentonite surface decreases from -44.9 to -31.6 mV. Interestingly, after hot rolling for 16 h at 180 °C, the negative charge on the bentonite surface further decreases. When the NaCl concentration is changed from 0 to 10 wt%, the zeta potential of bentonite increases from -38.2 to -25.5 mV. This shows that high temperature and high salt concentration synergistically reduce the negative charge on the surface of bentonite in the drilling fluid. As a result, the bentonite particles coalesce, destroying the grid structures formed among these particles in the drilling fluid. The rheology and lifting capacity of the drilling fluid are lost, thereby resulting in failure.

3.2. Filtration properties of drilling fluids at high temperature and high salinity

Apart from damaging the grid structure in the drilling fluid, which leads to the degradation the rheology and lifting performance, does the coalescence of bentonite particles affect other drilling fluid properties? It is not difficult to conjecture, bentonite particles are prone to coalesce, thus increasing the particle size under high temperature and high salt conditions. These large particles affect the thickness and compactness of the mud cake formed; eventually, fluid loss from the drilling fluid is induced.

The effect of salt on fluid loss is shown in Fig. 5a. At 25 °C, the fluid loss from the drilling fluid of 4% bentonite increases with the amount of NaCl. When NaCl concentration increases from 0 to 10 wt%, the fluid loss increases from 23.6 to 130.4 mL, indicating that the addition of NaCl considerably increases fluid loss. This is because NaCl reduces the negative charge on the surface of bentonite particles in the drilling fluid and causes these particles to coalesce, thus destroying the mud cake compactness. The effect of high temperature and high salt concentration on fluid loss is shown in Fig. 5b. After hot rolling for 16 h at 180 °C, the filtrations of 4% bentonite, 4% bentonite +5% NaCl, and 4% bentonite +10% NaCl are further increased to 52.0, 160.2, and 264.6 mL, respectively. The foregoing indicates that high temperature and high salt conditions promote fluid loss from the drilling fluid. This is because these conditions further reduce the negative charge on the surface of bentonites in the drilling fluid, causing the coalescence of bentonite

particles and deteriorating the mud cake compactness. After the addition of 0.05% carbon nanotube, the fluid loss from the drilling fluid is significantly reduced. For example, the filtration of drilling fluid of 4% bentonite +10% NaCl +0.05% carbon nanotube is reduced by 30.2%. This indicates that the addition of carbon nanotube can effectively reduce the filtration of drilling fluid at high temperatures and render the fluid suitable for an environment with high temperature and high salt concentration. This is because the carbon nanotube can increase the grid hindrance among bentonite particles by adsorbing on the surface of these particles. In turn, the fine particle size of bentonites is effectively maintained allowing them to form a dense mud cake under high temperature and high salt conditions.

The core soaking experiment is carried out by direct immersing the samples under normal temperature and pressure conditions. Core C was immersed in 4% bentonite+10% NaCl drilling fluid, and core F was immersed in 4% bentonite+10% NaCl+0.05% carbon nanotube drilling fluid. Before the immersion experiment, both drilling fluids were heated at 180 °C for 16 h. The NMR analysis results of cores C and F (which have similar permeabilities) after soaking in different drilling fluids are shown in Fig. 6. The cores C and F are two consecutive sections cut on the same core, the core size is 25 mm × 30 mm, and the gas permeability is 9.0 md and 9.1 md, respectively. T2 is the lateral relaxation time of the fluid phase in the core. The value of T2 represents the pore and throat sizes in the core. The amplitude represents the fluid content in the pore. The color bar on the right indicates different water saturations. Red represents 100% water content in the pores, while blue represents 0% water content. The peak area of T2 in core C is 1.86 times that in core F, and a considerable part of the image of core C is distinctively green compared with core F, which is slightly green in colour. These indicate that the amount of water that has penetrated core F is small, whereas more water has entered into core C. Core F is immersed in the drilling fluid with carbon nanotube, which means that the addition of carbon nanotubes can significantly reduce the entry of drilling fluid filtrate into the core under high temperature and high salt conditions. When carbon nanotubes adsorb on the surface of bentonite particles, the grid hindrance among bentonite particles is increased, the small size distribution of bentonite is maintained, a dense mud cake on the core surface is formed, the amount of filtrate that penetrates the core is reduced, and the wellbore wall in the deep formation is stabilised.

The change in bentonite particle size in drilling fluids under high temperature and high salt conditions is verified by the particle size

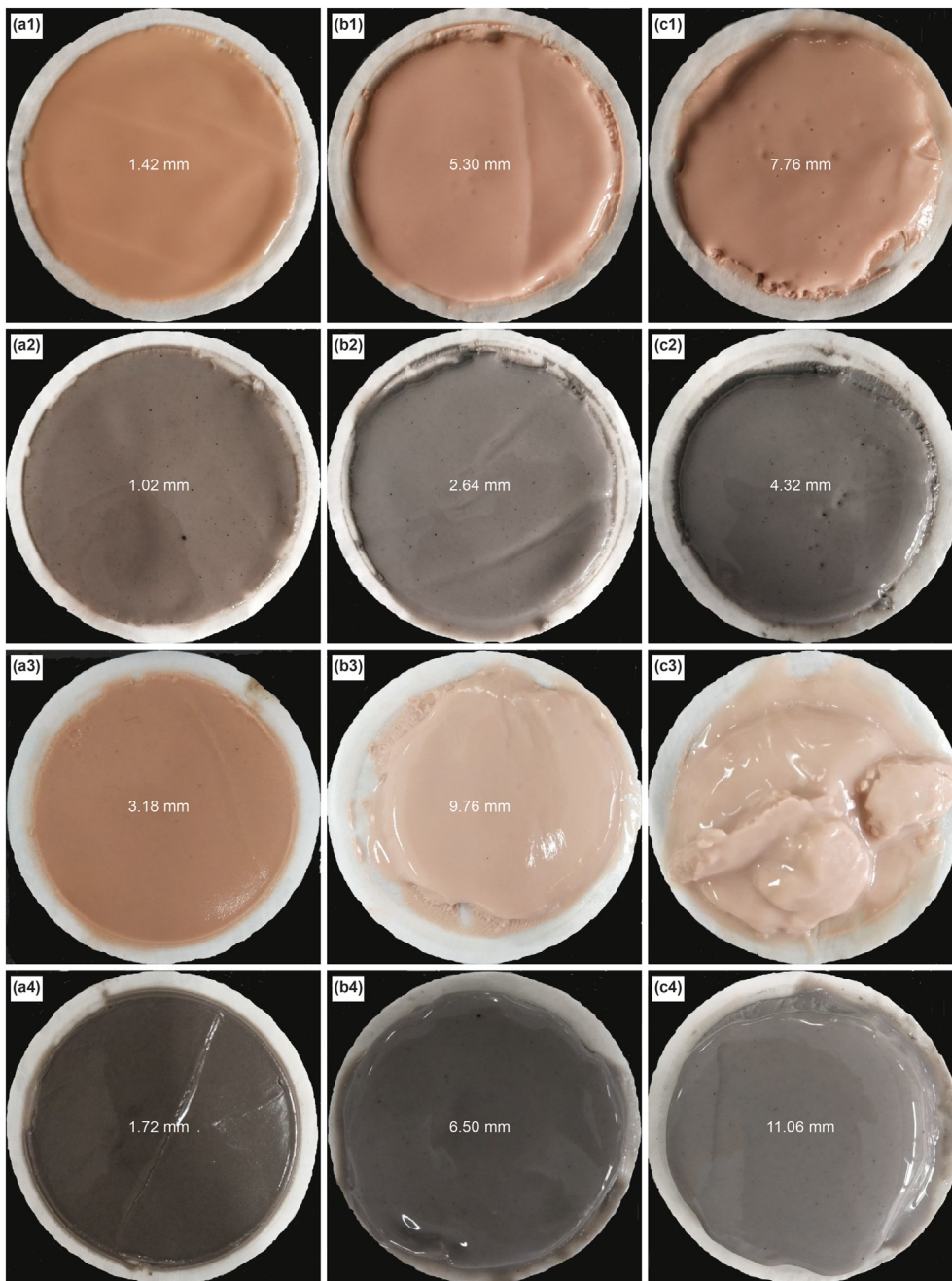


Fig. 8. Thickness and morphology of drilling fluid cake at 25 °C (a, 4% bentonite; b, 4% bentonite + 5% NaCl; c, 4% bentonite + 10% NaCl; a₂, 4% bentonite + 0.05% carbon nanotube; b₂, 4% bentonite + 5% NaCl + 0.05% carbon nanotube; c₂, 4% bentonite + 10% NaCl + 0.05% carbon nanotube). Thickness and morphology of drilling fluid cake after hot rolling for 16 h at 180 °C (a₃, 4% bentonite; b₃, 4% bentonite + 5% NaCl; c₃, 4% bentonite + 10% NaCl; a₄, 4% bentonite + 0.05% carbon nanotube; b₄, 4% bentonite + 5% NaCl + 0.05% carbon nanotube; c₄, 4% bentonite + 10% NaCl + 0.05% carbon nanotube).

experiment shown in Fig. 7. At 25 °C, the particle size of bentonite in the drilling fluid increases significantly with the presence 5 wt% NaCl compared with that in the drilling fluid with no NaCl. When the addition of NaCl is increased to 10 wt%, the particle size of bentonite increases further. After the addition of carbon nanotubes into the drilling fluid, however, the particle size is significantly reduced. After hot rolling for 16 h at 180 °C, the bentonite particle size significantly increases in the three drilling fluids (i.e., 4% bentonite, 4% bentonite + 5% NaCl, and 4% bentonite + 10% NaCl) compared with that at 25 °C. This is because the coalescence among bentonite particles in the drilling fluid is more severe under high

temperature and high salt conditions. After the addition of carbon nanotubes to the three drilling fluids, the increase in bentonite particle size is clearly inhibited. The carbon nanotubes adsorb on the bentonite surface, increase the grid hindrance, and effectively inhibit the coalescence of bentonite particles under high temperature and high salt conditions. Finally, the small particle size distribution in the drilling fluid is maintained.

In the drilling process, the mud cake mainly prevents water in the drilling fluid from entering the formation, thereby stabilising the well wall. Bentonite is directly involved in mud cake formation. The size difference among bentonite particles in the drilling fluid is

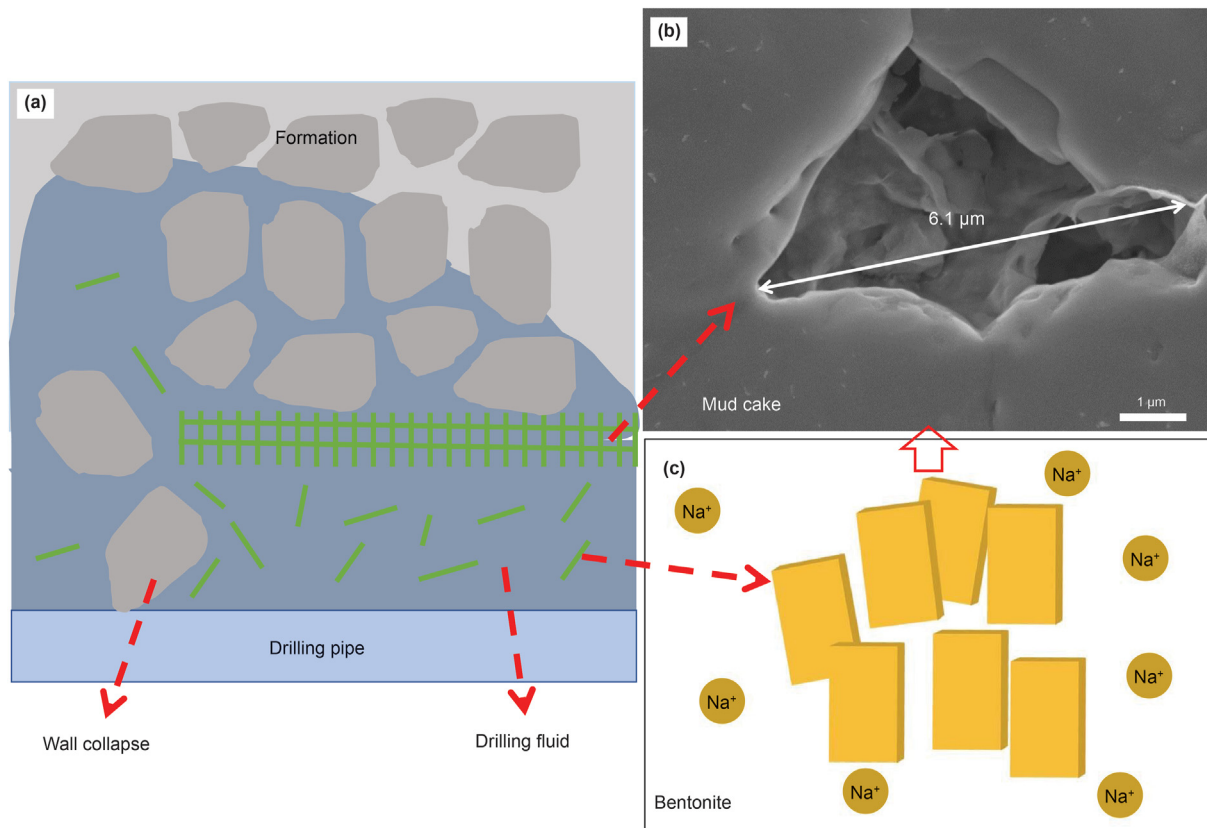


Fig. 9. Wellbore instability caused by failure of drilling fluid under high temperature and high salt conditions. (a) the wall collapse due to the intrusion of the drilling fluid into the formation through the large pores in the loose mud cake; (b) SEM images of cakes of 4% bentonite + 10% NaCl after hot rolling for 16 h at 180 °C; (c) bentonites in the drilling fluid of 4% bentonite + 10% NaCl at 180 °C).

large, and the differences among the mud cakes formed by these particles are evident, as shown in Fig. 8. At 25 °C, as the amount of NaCl increases, the thicker the mud cake becomes. The mud cake formed by drilling fluids that contain carbon nanotubes is significantly thinner because it is formed by small bentonite particles, whereas that formed by large bentonite particles is thick.

After hot rolling for 16 h at 180 °C, the mud cakes formed by the six drilling fluids are thicker than those formed at 25 °C, especially for drilling fluid of 4% bentonite + 10% NaCl it cannot form integrated mud cake (Fig. 8c₃), which could not even form a complete mud cake. The mud cake formed by the drilling fluid containing carbon nanotubes is significantly thinner and intact, indicating that carbon nanotubes can effectively inhibit the thickening of mud cake under high temperature and high salt conditions and maintain the integrity of the cake.

The size of bentonite particles also affects mud cake compactness, which in turn affects the cake's ability to prevent water from entering the formation. High temperature and high salt concentration synergistically coalesce the bentonite particles (Fig. 9c) and destroy the grid structure formed among bentonite particles in the drilling fluid, thereby destroying the drilling fluid's rheology and lifting capacity. At the same time, when bentonite particles become larger, fluid loss from the drilling fluid increases. As shown in Fig. 9b, when 10% NaCl is added to the drilling fluid of 4% bentonite, pores with a size of 6.1 μm appear in the mud cake. The mud cake formed by the accumulation of large bentonite particles is loose; hence, the pores in the mud cake are larger, and more filtration enters the formation through the pores, causing the collapse of the wellbore (Fig. 9a).

The pore size in the mud cake formed by the drilling fluid

containing carbon nanotubes is greatly reduced, however, and it is difficult to observe these pores clearly (Fig. 10b). This indicates that carbon nanotubes can effectively maintain the density of the mud cake formed by the drilling fluid under high temperature and high salt conditions. The foregoing is mainly related to the fact that carbon nanotubes can effectively maintain the small size of bentonite particles under high temperature and high salt conditions. The mud cake is relatively dense because the gap formed by the accumulation of small-sized bentonite particles is small. The adsorption of carbon nanotubes on the surface of bentonite particles increases the steric hindrance among bentonite particles and maintains the small particle size of bentonite under high temperature and high salt conditions (Fig. 10c). This supports the bentonite grid structure in the drilling fluid and forms a dense mud cake. In turn, these maintain the rheology and lifting performance of the drilling fluid and reduce the filtration of drilling fluid; accordingly, the drilling fluid can be applied to deep formation drilling even under high temperature and high salt conditions (Fig. 10a).

4. Conclusion

In this work, our study reveals the failure mechanism of water-based drilling fluid under high temperature and high salt conditions. High temperature and salinity reduce the negative charge on the surface of bentonite in the drilling fluid and cause the coalescence of bentonite particles. As a result, the particles coalesce, the grid structure is destroyed, and the rheological properties, rock-carrying capacity and filtration properties are lost. In addition, a drilling fluid stabilization technique in the presence of NaCl with a 10 wt% concentration at a temperature of 180 °C is developed by

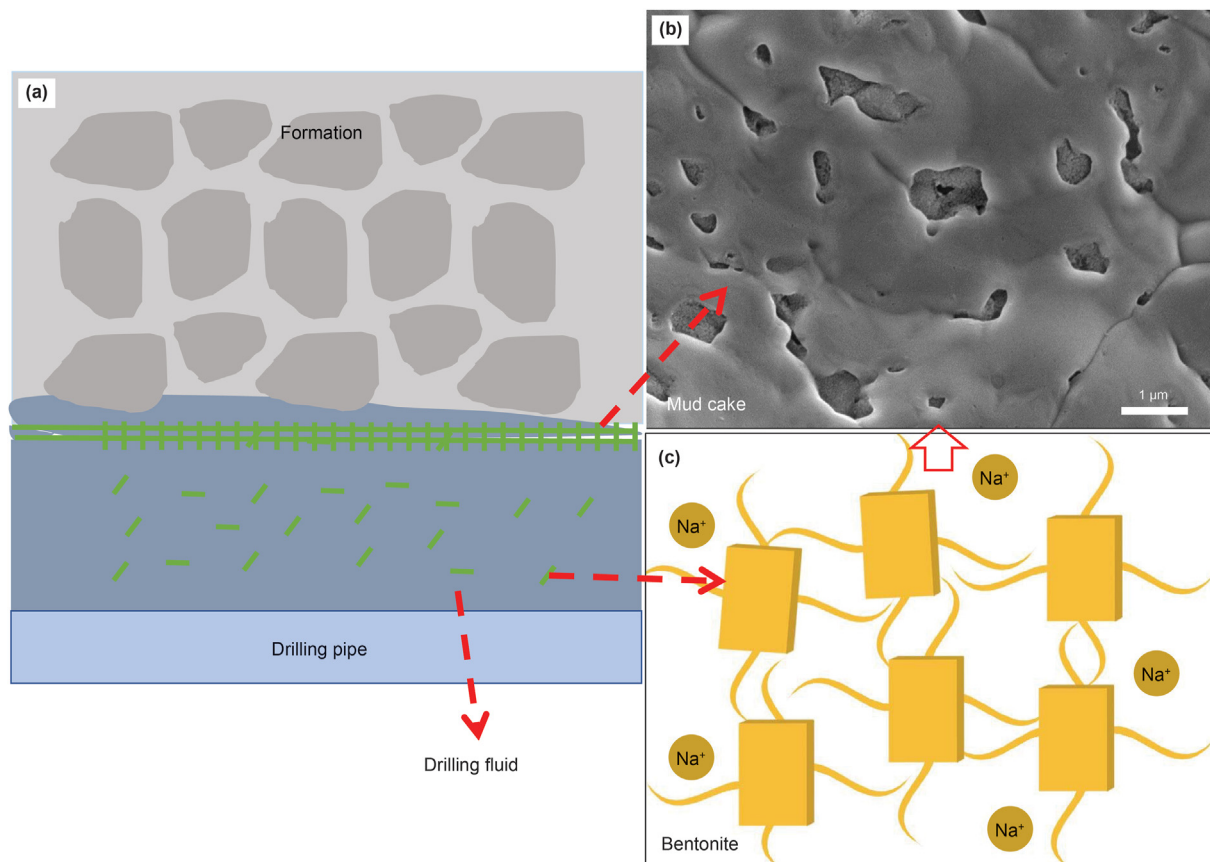


Fig. 10. Temperature and salt tolerance mechanism of drilling fluid with carbon nanotube additive. (a) stable wall under the protection of dense mud cake formed by the accumulation of small-sized bentonite particles; (b) SEM images of cakes of 4% bentonite + 10% NaCl + 0.05% carbon nanotube after hot rolling for 16 h at 180 °C; (c) bentonites in drilling fluids with 10% NaCl and 0.05% carbon nanotube at 180 °C.

introducing 0.05 wt% carbon nanotubes into a 4% bentonite fluid. As a result, the rock-carrying capacity of the drilling fluid increases by 85.1%, and the filtration of bentonite drilling fluid reduces by 30.2%. The new drilling fluid is able to support the exploration and development of hydrocarbon resources in deep formations with high temperature and high salt concentration.

Acknowledgments

This research was financially supported by the Natural Science Foundation of China (Grants 51904328), the Natural Science Foundation of China (Grants U1762212) and Fundamental Research Funds for the Central Universities (Grants 27R1702031A).

References

- Aftab, A., Ismail, A.R., Ibupotod, Z.H., et al., 2017. Nanoparticles based drilling muds a solution to drill elevated temperature wells: a review. *Renew. Sustain. Energy Rev.* 76, 1301–1313. <https://doi.org/10.1016/j.rser.2017.03.050>.
- Amin, K.B., Hasan, H.S., 2018. Rheological investigation of smart polymer/carbon nanotube complex on properties of water-based drilling fluids. *Colloids Surf., A* 556, 23–29. <https://doi.org/10.1016/j.colsurfa.2018.07.058>.
- Anderson, A., Rezaie, B., 2019. Geothermal technology: trends and potential role in a sustainable future. *Appl. Energy* 248, 18–34. <https://doi.org/10.1016/j.apenergy.2019.04.102>.
- Babaei, M., Hamidreza, M.N., 2019. Performance of low-enthalpy geothermal systems: interplay of spatially correlated heterogeneity and well-doublet spacings. *Appl. Energy* 253, 113569. <https://doi.org/10.1016/j.apenergy.2019.113569>.
- Baltoiu, L.V., Warren, B.K., Natros, T., 2008. State-of-the-Art in coalbed methane drilling fluids. *SPE Drill. Complet.* 23, 250–257. <https://doi.org/10.2118/101231-PA>.
- Bera, A., Belhaj, H., 2016. Application of nanotechnology by means of nanoparticles and nanodispersions in oil recovery-A comprehensive review. *J. Nat. Gas Sci. Eng.* 34, 1284–1309. <https://doi.org/10.1016/j.jngse.2016.08.023>.
- Benayada, B., Habchi, K.N., Khodja, M., 2003. Stabilisation of clay walls during drilling in southern Algeria. *Appl. Energy* 75, 51–59. [https://doi.org/10.1016/S0306-2619\(03\)00018-7](https://doi.org/10.1016/S0306-2619(03)00018-7).
- Cao, J., Meng, L., Yang, Y.P., et al., 2017. Novel Acrylamide/2-acrylamide-2-methylpropanesulfonic acid/4-vinylpyridine terpolymer as an anti-calcium contamination fluid-Loss additive for water-based drilling fluids. *Energy Fuels* 31, 11963–11970. <https://doi.org/10.1021/acs.energyfuels.7b02354>.
- Chen, L., Xu, G.Y., Rui, Z.H., et al., 2019. Demonstration of a feasible energy-water-environment nexus: waste sulfur dioxide for water treatment. *Appl. Energy* 250, 1011–1022. <https://doi.org/10.1016/j.apenergy.2019.05.108>.
- Chu, Q., Luo, P., Zhao, Q.F., et al., 2013. Application of a new family of organosilicon quadripolymer as a fluid loss additive for drilling fluid at high temperature. *J. Appl. Polym. Sci.* 128, 28–40. <https://doi.org/10.1002/app.38096>.
- Cui, G., Rui, Z., Pei, S., et al., 2020. Whole process analysis of geothermal exploitation and power generation from a depleted high-temperature gas reservoir by recycling CO₂. *Energy*. <https://doi.org/10.1016/j.energy.2020.119340>.
- De Silva, G.P.D., Ranjith, P.G., Perera, M.S.A., et al., 2016. Effect of bedding planes, their orientation and clay depositions on effective re-injection of produced brine into clay rich deep sandstone formations: implications for deep earth energy extraction. *Appl. Energy* 161, 24–40. <https://doi.org/10.1016/j.apenergy.2015.09.079>.
- Dias, F.T.G., Souza, R.R., Lucas, E.F., 2015. Influence of modified starches composition on their performance as fluid loss additives in invert-emulsion drilling fluids. *Fuel* 140, 711–716. <https://doi.org/10.1016/j.fuel.2014.09.074>.
- Emmanuel, U.A., Godpower, C.E., Ghasem, N., et al., 2019. Water-based drilling fluids for high-temperature applications and water-sensitive and dispersible shale formations. *J. Petrol. Sci. Eng.* 175, 1028–1038. <https://doi.org/10.1016/j.petrol.2019.01.002>.
- Fu, L.P., Liao, K.L., Ge, J.J., 2020. Study on the damage and control method of fracturing fluid to tight reservoir matrix. *J. Nat. Gas Sci. Eng.* 82, 103464. <https://doi.org/10.1016/j.jngse.2020.103464>.
- Guo, J.K., Yan, J.N., Fan, W.W., et al., 2006. Applications of strongly inhibitive silicate-based drilling fluids in troublesome shale formations in Sudan. *J. Petrol. Sci. Eng.* 50, 195–203. <https://doi.org/10.1016/j.petrol.2005.12.006>.
- Guo, T., Tang, S., Liu, S., et al., 2020. Physical simulation of hydraulic fracturing of

- large-sized tight sandstone outcrops. *SPE J.* <https://doi.org/10.2118/204210-PA>.
- He, Y., Cheng, S., Sun, Z., et al., 2020. Improving oil recovery through fracture injection and production of multiple fractured horizontal wells. *J. Energy Resour. Technol.* 142 (5), 053002. <https://doi.org/10.1115/1.4045957>.
- Huang, W.A., Li, X., Qiu, Z.S., et al., 2017. Inhibiting the surface hydration of shale formation using preferred surfactant compound of polyamine and twelve alkyl two hydroxyethyl amine oxide for drilling. *J. Petrol. Sci. Eng.* 159, 791–798. <https://doi.org/10.1016/j.petrol.2017.10.006>.
- Hunter, R.J., Alexander, A.E., 1963. Surface properties and flow behavior of kaolinite. part III: flow of kaolinite sols through a silica column. *J. Colloid Sci.* 18, 846–862. [https://doi.org/10.1016/0095-8522\(63\)90078-3](https://doi.org/10.1016/0095-8522(63)90078-3).
- Jalal, A.A., Hawazin, K.M., Dania, F.A., et al., 2020. Analytical water saturation model using capacitance-resistance simulation: clean and shaly formations. *J. Nat. Gas Sci. Eng.* 82, 103225. <https://doi.org/10.1016/j.jngse.2020.103325>.
- Jia, H., Huang, P., Wang, Q.X., et al., 2019. Investigation of inhibition mechanism of three deep eutectic solvents as potential shale inhibitors in water-based drilling fluids. *Fuel* 244, 403–411. <https://doi.org/10.1016/j.fuel.2019.02.018>.
- Jung, Y., Son, Y.H., Lee, J.K., et al., 2011. Rheological behavior of clay–nanoparticle hybrid-added bentonite suspensions: specific role of hybrid additives on the gelation of clay-based fluids. *ACS Appl. Mater. Interfaces* 3, 3515–3522. <https://doi.org/10.1021/am200742b>.
- Kelessidis, V.C., Poulakakis, E., Chatzistamou, V., 2011. Use of carboxypol 980 and carboxymethyl cellulose polymers as rheology modifiers of sodium-bentonite water dispersions. *Appl. Clay Sci.* 54, 63–69. <https://doi.org/10.1016/j.clay.2011.07.013>.
- Li, K., Khanna, R., Zhang, J., et al., 2015a. Comprehensive investigation of various structural features of bituminous coals using advanced analytical techniques. *Energy Fuel* 29, 7178–7189. <https://doi.org/10.1021/acs.energyfuels.5b02064>.
- Li, M.C., Wu, Q., Song, K., et al., 2015b. Cellulose nanoparticles as modifiers for rheology and fluid loss in bentonite water-based fluids. *ACS Appl. Mater. Interfaces* 7, 5006–5016. <https://doi.org/10.1021/acsami.5b00498>.
- Li, X.S., Xu, C.G., Zhang, Y., et al., 2016. Investigation into gas production from natural gas hydrate: a review. *Appl. Energy* 172, 286–322. <https://doi.org/10.1016/j.apenergy.2016.03.101>.
- Li, Y., Xu, L., Gong, H.J., et al., 2017. A microbial copolysaccharide produced by sphingomonas species for enhanced heavy oil recovery at high temperature and high salinity. *Energy Fuels* 34, 3960–3969. <https://doi.org/10.1021/acs.energyfuels.6b02923>.
- Liu, J.P., Dai, Z.W., Li, C.J., et al., 2019a. Inhibition of the hydration expansion of sichuan gas shale by adsorption of compounded surfactants. *Energy Fuels* 33, 6020–6026. <https://doi.org/10.1021/acs.energyfuels.9b00637>.
- Liu, J.P., Dai, Z.W., Xu, K., et al., 2020. Water-based drilling fluid containing bentonite/poly (sodium 4-styrenesulfonate) composite for ultrahigh-temperature ultra-deep drilling and its field performance. *SPE J.* 25 (3), 1193–1202. <https://doi.org/10.2118/199362-PA>.
- Liu, J.R., Sheng, J.J., 2019. Experimental investigation of surfactant enhanced spontaneous imbibition in Chinese shale oil reservoirs using NMR tests. *J. Ind. Eng. Chem.* 75, 414–422. <https://doi.org/10.1016/j.jiec.2018.12.044>.
- Liu, Y., Chen, S., Guan, B., et al., 2019b. Layout optimization of large-scale oil-gas gathering system based on combined optimization strategy. *Neurocomputing* 332, 159–183. <https://doi.org/10.1016/j.neucom.2018.12.021>.
- Luckham, P.F., Rossi, S., 1999. The colloidal and rheological properties of bentonite suspensions. *Adv. Colloid Interface Sci.* 82, 43–92. [https://doi.org/10.1016/S0001-8686\(99\)00005-6](https://doi.org/10.1016/S0001-8686(99)00005-6).
- Luo, Z.H., Pei, J.G., Wang, L.X., et al., 2017. Influence of an ionic liquid on rheological and filtration properties of water-based drilling fluids at high temperatures. *Appl. Clay Sci.* 136, 96–102. <https://doi.org/10.1016/j.clay.2016.11.015>.
- Maury, V., Guenot, A., 1995. Practical advantages of mud cooling systems for drilling. *SPE Drill. Complet.* 10, 42–48. <https://doi.org/10.2118/25732-pa>.
- Menezes, R.R., Marques, L.N., Campos, L.A., et al., 2010. Use of statistical design to study the influence of CMC on the rheological properties of bentonite dispersions for water-based drilling fluids. *Appl. Clay Sci.* 49, 13–20. <https://doi.org/10.1016/j.clay.2010.03.013>.
- Pandey, S., Vishal, V., 2017. Sensitivity analysis of coupled processes and parameters on the performance of enhanced geothermal systems. *Sci. Rep.* 7, 17057. <https://doi.org/10.1038/s41598-017-14273-4>.
- Saeid, S., Al-Khoury, R., Nick, H.M., et al., 2018. A prototype design model for deep low-enthalpy hydrothermal systems. *Renew. Energy* 77, 408–422. <https://doi.org/10.1016/j.renene.2014.12.018>.
- Salami, O.T., Plank, J., 2013. Preparation and properties of a dispersing fluid loss additive based on humic acid graft copolymer suitable for cementing high temperature (200 °C) oil wells. *J. Appl. Polym. Sci.* 129, 2544–2553. <https://doi.org/10.1002/app.38980>.
- Sehly, K., Chiew, H.L., Li, H., et al., 2015. Stability and ageing behaviour and the formulation of potassium-based drilling muds. *Appl. Clay Sci.* 104, 309–317. <https://doi.org/10.1016/j.clay.2014.12.013>.
- Seright, R.S., Henrici, B.J., 1990. Xanthan stability at elevated temperatures. *SPE Reservoir Eng.* 5, 56–60. <https://doi.org/10.2118/14946-PA>.
- Shan, W.J., Tao, S.X., Fu, F., et al., 2014. Research on the drilling fluid technology for high temperature over 240°C. *Process Eng.* 73, 218–229. <https://doi.org/10.1016/j.proeng.2014.06.191>.
- Shortall, R., Davidsdottir, B., Axelsson, G., 2015. Geothermal energy for sustainable development: a review of sustainability impacts and assessment frameworks. *Renew. Sustain. Energy Rev.* 44, 391–406. <https://doi.org/10.1016/j.rser.2014.12.020>.
- Tang, Y., Hou, C., He, Y., et al., 2020. Review on pore structure characterization and microscopic flow mechanism of CO2 flooding in porous media. *Energy Technol.* <https://doi.org/10.1002/ente.202000787>.
- Tiemeyer, C., Plank, J., 2013. Synthesis, Characterization, and working mechanism of a synthetic high temperature (200 °C) fluid loss polymer for oil well cementing containing allyloxy-2-hydroxy propane sulfonic (AHPS) acid monomer. *J. Appl. Polym. Sci.* 128, 851–860. <https://doi.org/10.1002/app.38262>.
- Timon, E., Johann, P., 2019. An improved test protocol for high temperature carrying capacity of drilling fluids exemplified on a sepiolite mud. *J. Nat. Gas Sci. Eng.* 70, 102964. <https://doi.org/10.1016/j.jngse.2019.102964>.
- Tokimatsu, K., Höök, M., McLellan, B., et al., 2018. Energy modeling approach to the global energy-mineral nexus: exploring metal requirements and the well-below 2 °C target with 100 percent renewable energy. *Appl. Energy* 225, 1158–1175. <https://doi.org/10.1016/j.apenergy.2018.05.047>.
- Vedachalam, N., Ramesh, S., Srinivasalu, S., et al., 2016. Assessment of methane gas production from Indian gas hydrate petroleum systems. *Appl. Energy* 168, 649–660. <https://doi.org/10.1016/j.apenergy.2016.01.117>.
- Vikas, M., Rajat, J., 2015. Evaluation of polyacrylamide/clay composite as a potential drilling fluid in inhibitive water-based fluid system. *J. Petrol. Sci. Eng.* 133, 612–621. <https://doi.org/10.1016/j.petrol.2015.07.009>.
- Wellington, S.L., 1983. Biopolymer solution viscosity stabilisation – polymer degradation and antioxidant use. *Soc. Petrol. Eng. J.* 23, 901–912. <https://doi.org/10.2118/9296-PA>.
- Willems, C., Nick, H., Goense, T., et al., 2017. The impact of reduction of doublet well spacing on the net present value and the life time of fluvial hot sedimentary aquifer doublets. *Geothermics* 68, 54–66. <https://doi.org/10.1016/j.geothermics.2017.02.008>.
- Wu, B., Zhang, X., Jeffrey, R.G., 2014. A model for downhole fluid and rock temperature prediction during circulation. *Geothermics* 50, 202–212. <https://doi.org/10.1016/j.geothermics.2013.10.004>.
- Xu, J., Tang, H., Su, S., et al., 2018. A study of the relationships between coal structures and combustion characteristics: the insights from micro-Raman spectroscopy based on 32 kinds of Chinese coals. *Appl. Energy* 212, 46–56. <https://doi.org/10.1016/j.apenergy.2017.11.094>.
- Yang, M., Luo, D.Y., Chen, Y.H., et al., 2019. Establishing a practical method to accurately determine and manage wellbore thermal behavior in high-temperature drilling. *Appl. Energy* 238, 1471–1483. <https://doi.org/10.1016/j.apenergy.2019.01.164>.
- Yang, X.Y., Shang, Z.X., Shi, Y.P., et al., 2018. Influence of salt solutions on the permeability, membrane efficiency and wettability of the Lower Silurian Longmaxi shale in Xiushan, Southwest China. *Appl. Clay Sci.* 158, 83–93. <https://doi.org/10.1016/j.clay.2018.02.006>.
- Yao, L.J., Anne, N.M., Jobson, A., 2015. Soil microbial response to waste potassium silicate drilling fluid. *J. Environ. Sci. (China)* 29, 189–198. <https://doi.org/10.1016/j.jes.2014.10.007>.
- Yekeen, N., Padmanabhan, E., Idris, A.K., et al., 2019. Surfactant adsorption behaviors onto shale from Malaysian formations: influence of silicon dioxide nanoparticles, surfactant type, temperature, salinity and shale lithology. *J. Petrol. Sci. Eng.* 179, 841–854. <https://doi.org/10.1016/j.petrol.2019.04.096>.
- Yu, H.Y., Rui, Z.H., Chen, Z.W., et al., 2019. Feasibility study of improved unconventional reservoir performance with carbonated water and surfactant. *Energy* 182, 135–147. <https://doi.org/10.1016/j.energy.2019.06.024>.